



Multiplexing T- and B-Cell FLUOROSPOT Assays: Experimental Validation of the Multi-Color ImmunoSpot® Software Based on Center of Mass Distance Algorithm

**Alexey Y. Karulin, Zoltán Megyesi, Richard Caspell, Jodi Hanson,
and Paul V. Lehmann**

Abstract

Over the past decade, ELISPOT has become a highly implemented mainstream assay in immunological research, immune monitoring, and vaccine development. Unique single cell resolution along with high throughput potential sets ELISPOT apart from flow cytometry, ELISA, microarray- and bead-based multiplex assays. The necessity to unambiguously identify individual T and B cells that do, or do not co-express certain analytes, including polyfunctional cytokine producing T cells has stimulated the development of multi-color ELISPOT assays. The success of these assays has also been driven by limited sample/cell availability and resource constraints with reagents and labor. There are few commercially available test kits and instruments available at present for multi-color FLUOROSPOT. Beyond commercial descriptions of competing systems, little is known about their accuracy in experimental settings detecting individual cells that secrete multiple analytes vs. random overlays of spots. Here, we present a theoretical and experimental validation study for three and four color T- and B-cell FLUOROSPOT data analysis. The ImmunoSpot® Fluoro-X™ analysis system we used includes an automatic image acquisition unit that generates individual color images free of spectral overlaps and multi-color spot counting software based on the maximal allowed distance between centers of spots of different colors or Center of Mass Distance (COMD). Using four color B-cell FLUOROSPOT for IgM, IgA, IgG1, IgG3; and three/four color T-cell FLUOROSPOT for IL-2, IFN- γ , TNF- α , and GzB, in serial dilution experiments, we demonstrate the validity and accuracy of Fluoro-X™ multi-color spot counting algorithms. Statistical predictions based on the Poisson spatial distribution, coupled with scrambled image counting, permit objective correction of true multi-color spot counts to exclude randomly overlaid spots.

Key words ELISPOT, FLUOROSPOT, Polyfunctional, T cell, B cell, Immunoglobulin, Antibody, Cytokine, Center of mass, ImmunoSpot®, Fluoro-X™, Software, Fluorescence, Multi-color, Multiplex, Spot counting, Image analysis

1 Introduction

Dual-color ELISPOT assays based on traditional enzyme-tagged reagents and two to three color FLUOROSPOT assays based on fluorophore-tagged reagents have become increasingly popular in

immunological research and immune monitoring. Recently, four color T-cell and seven color B-cell assays have also become commercially available. A number of commercial vendors now offer test kits and automated spot counters for simultaneous detection of various biological molecules secreted by activated T and B lymphocytes and other immune cells. There are two main reasons for multiplexing ELISPOT assays. First reason is purely pragmatic: detection of several analytes secreted by T or B cells in a single culture well reduces both the labor and the amount of cells/reagents required, and thus proportionally reduces the cost to perform the assay. Beyond cost, in clinical settings primary cells are frequently limited and quality controlled reagents also may be limited in the context of novel analytes. Secondly, it is increasingly clear that monitoring polyfunctional T-cell secreting multiple cytokines in various combinations at a time (like IL-2/IFN- γ or IL2/GzB/TNF- α) provides better assessment of protective immunity [1–13]. Although the procedural steps in performing multi-color cytokine (or antibody) FLUOROSPOT is not significantly different from a single-color ELISPOT, analyzing the results obtained, i.e., the spots with more than two colors, is a complex image analysis challenge. In case of FLUOROSPOT complex color recognition task can be reduced to a single-color analysis of separate single-color images generated for each individual analyte with subsequent detection of dual-/triple-/multi-color spots occupying the same location on the membrane. Such images can be readily generated using individual combinations of excitation/emission filters (fluorescent channel) optimized for each fluorochrome. The remaining issue is to develop an algorithm for accurately matching or “pairing” single-color spots from individual fluorescent channels to identify dual-, triple-, or multi-color spots. In the ImmunoSpot[®] Software v. 5.0 (September 2010 by CTL, Cleveland OH), we introduced a Center of Mass Distance algorithm based on the maximal allowed distance between centers of spots in individual color images. For bright fluorescence spots on a dark background, this “center of mass” corresponds to the center of light intensity inside the spot outline (often referred to in image analysis as “center of gray”). We found that due to several reasons discussed below, centers of gray (referred to as centers of mass from hereon) for individual colors never coincide precisely for true multi-color spots. To account for these color “shifts,” we included a maximal allowed distance (in ImmunoSpot[®] Software, it is called Center of Mass Distance or COMD) parameter, which depends on the optical characteristics of a reader and specific fluorescent labels used. From the user perspective, any algorithm used for FLUOROSPOT multi-color image analysis is a “black box” and has to be validated. In this study, we propose an experimental validation approach based on two independent assays. One uses a four color B-cell FLUOROSPOT for

human Ig classes and subclasses where no dual- or multi-color spots are possible due to allelic exclusion. The second assay is a three and four color T-cell FLUOROSPOT detecting analytes that T cells are known to co-express. Using statistical predictive approach and scrambled (distorted) spot positions, we are able to differentiate closely situated cells producing different cytokines, from a single cell producing multiple cytokines at a time.

2 Materials

1. Human cryopreserved PBMC of 2 HLA-A2-positive donors were obtained from our commercial ePBMC[®] library (CTL, Shaker Heights, OH). These PBMC had been previously HLA-typed at high resolution and characterized for T-cell reactivity to a variety of antigens previously (details are available at <http://www.immunospot.com/ImmunoSpot-ePBMC>).
2. Human IFN- γ /TNF- α /GzB (<http://www.immunospot.com/immunospot-kits/human-interferon-gamma-tnf-a-granzyme-b-three-color-fluorospot>) and IFN- γ /TNF- α /IL-2 (<http://www.immunospot.com/immunospot-kits/human-interferon-gamma-tnf-a-il-2-three-color-fluorospot>) FLUOROSPOT three color kits were obtained from CTL (Shaker Heights, OH).
3. Human four color B-cell FLUOROSPOT kit for simultaneous detection of total IgM, IgA, IgG1, and IgG3 producing cells (<http://www.immunospot.com/immunospot-kits/human-igm-iga-igg1-igg3-four-color-fluorospot>, CTL, Shaker Heights, OH).
4. FLUOROSPOT plates were scanned and analyzed using an ImmunoSpot[®] S6-Ultimate UV Reader (CTL, Shaker Heights, OH). Single-/dual-/multi-color spots were counted automatically by using the ImmunoSpot[®] v.7.0 Fluoro-X[™] Software Suite (CTL, Shaker Heights, OH) as described in the Methods Subheadings 3.7 and 3.8.

3 Methods

3.1 Cell Preparation

Prior to testing, the PBMC cryo-vials, stored in the liquid N₂ vapor phase, were transferred to dry ice in styrofoam containers for transport to and short-term storage in the laboratory. Then the cells were thawed essentially following a protocol providing the optimal functionality and recovery for cryopreserved PBMC [14]. Specifically, cryo-vials were rapidly warmed up to 37 °C in the glass bead bath (CTL-BB-001, for 8 min at 37 °C). Warmed up cryo-vials were flipped twice to re-suspend the cells and the cell suspension (10 million cells in 1 mL) was gently transferred with a wide-bore 2-mL

pipette into a 15-mL V-bottom Falcon tube. For complete cell recovery, the cryo-vials were rinsed with 1 mL warm (37 °C) CTL Anti-Aggregate-Wash™ medium (CTL-AA-005) containing benzonase. An additional 8 mL CTL Anti-Aggregate-Wash™ warm medium (37 °C) was added to the 15-mL tube at a rate of 2 mL per every 5 s. PBMCs were counted by fluorescence microscopy using Acridine Orange and Ethidium Bromide (AO/EB), then washed twice in 10 mL CTL-Test™ warm medium (CTLT-005) and re-suspended at a final concentration of 3×10^6 /mL in the same medium. The freshly thawed PBMC (100 μ L) were plated (within 1 h) into an ELISPOT 96 well plate (Msn HTS IP, Millipore, MA, USA).

3.2 T-Cell FLUOROSPOT

T-cell assays were performed following the manufacturer's protocols. Antigens EBV-dominant HLA-A2 restricted peptide LMP2A (426–434) and HCMV HLA-A2 restricted peptide pp65 (495–503) (EZ Biolab Inc., Carmel, IN, USA) were plated in 100 μ L per well prior to cells into the capture antibody-coated assay plate. Final concentration of peptides was 1 μ g/mL. The antigens were dissolved in CTL-Test™ medium (CTLT-005). Same test medium (without antigen) was used as negative control. The plates containing the antigens (or medium controls) were kept at 37 °C in a CO₂ incubator until the cells were ready to be plated. Final concentration of PBMC was 3×10^5 /mL unless specified otherwise. In cell titration experiments, PBMC were diluted in CTL-test medium to the required concentrations and 100 μ L/well. PBMC were always plated using wide-bore pipette tips, after which plates were gently tapped on each side to ensure even distribution of the cells. For the duration of the assay (24 h), plates were incubated at 37 °C in a CO₂ incubator.

3.3 B-Cell FLUOROSPOT

For multi-color B-cell FLUOROSPOT, human PBMC were prepared as described above. Prior to the assay, B cells were polyclonally pre-activated with R848 and human rIL-2 [15]. After pre-activation, cells were washed once in CTL-Test-B™ medium and counted as described above. PBMC were tested in 2 \times serial dilutions from 10,000 down to 78 cells per well. Plates with cells were incubated 24 h at 37 °C in a CO₂ incubator. B-cell FLUOROSPOT kit was used according to the manufacturer's protocols and recommendations. As capture reagents, mouse monoclonal antibodies against human Ig light κ/λ chains were used. Following protocol specified washing and developing steps, plates were air dried in a laminar hood.

3.4 Theoretical Calculations of Random Spot Overlays Based on Statistical Predictions

Assuming that cells in the ELISPOT plate well are distributed on the surface of the membrane according to the Uniform distribution law (any position has equal chance to be occupied by the spot) and each cell produces only single analyte at a time (such as in case of B-cell ELISPOT), we can postulate that the probability for spots of different color to overlay randomly (creating “false” multi-color spot) will follow Poisson Point Process [16].

Let Center of Mass Distances (COMD) be the maximum allowed distance between centers of masses of spots of different colors to form a multi-color spot, then $A_{\text{thrs}} = \pi \text{COMD}^2$ will be the threshold area in the Poisson Point Process. Let N_i be the spot count/well of color i (for example, for blue $i = 1$, for red—2, red—3, and so on), A_{image} be the total well area, and $\lambda_i = N_i/A_{\text{image}}$ —the surface density of the color i spots. Let N_{ij} be the number of “false” dual-color spots containing colors i and j . According to the Poisson Point Processes, the probability that any well circular region A_{thrs} contains at least one spot of j color can be written as:

$$P_j \stackrel{\text{def}}{=} e^{-\lambda_j A_{\text{thrs}}} \quad (1)$$

Then the “false” dual-color count for spots containing colors i and j will be:

$$N_{ij} \stackrel{\text{def}}{=} N_i P_j \quad (2)$$

In the general form, the number of “false” multi-color spots containing color i can be written as:

$$N_{i,j..n} \stackrel{\text{def}}{=} N_i \prod_{k \in j..n} P_k \quad (3)$$

3.5 Monte Carlo Simulations

To prove our statistical predictions based on the Poisson Point Process, we used the Monte Carlo method [17]. Thousand artificial image sets were created with four colors in each. Random spots coordinates (center of mass positions) were generated using the uniform distribution independently for each of four colors. These artificial image sets were counted using standard Fluoro-X™ pairing algorithm (same way as real images are analyzed). Then the average numbers of dual-/multi-color spots were calculated among all sets. These simulations were repeated for different individual color spot numbers and different COMD.

3.6 Scrambled Image Counting

We also compare Poisson predictions with a method that can be applied on either artificial or real image sets. We refer to this method as “image scrambling.” Relative orientations of individual color, real-well images (or artificially generated images) were randomly changed (scrambled), then standard spot pairing was performed to count multi-color spots. As in case of Monte Carlo simulation, counting was repeated for different spot numbers and different COMD.

Both of the abovementioned methods generate counting results for “false” positive multi-color spots formed by random overlays of the single-color spots.

3.7 Analysis of Individual Color Spots in Multi-color FLUOROSPOT

Analyzing of multi-color spots using a color image is not feasible owing to several reasons. Fluorescence intensity of individual fluorochromes are not equal due to their spectral properties (mainly extinction coefficient and quantum yield), and therefore are not directly comparable on a unitary scale. Therefore different exposures are needed to generate suitable spot images for each fluorochrome. The level of each cytokine secretion could be also radically different. When all fluorochromes are excited simultaneously, the overlap of the emission spectra will not permit reliable detection; particularly, when more than two colors are used. Also excitation spectrum of one fluorochrome may overlap with the emission spectrum of another, thus limiting the choice of labels for multi-color assay. Exciting one label at a time using computer-controlled, LED-based color illuminator and asynchronous excitation/emission filter selector completely eliminates the problem of spectral overlap and cross contamination of fluorescence between channels (*see Note 1*). In a well-designed optical system, no compensation is required between individual color channels (Fig. 1). The figure shows data for a B-cell IgG FLUOROSPOT assay where no dual-/multi-color spots are possible.

Basic principles of single-color FLUOROSPOT image analysis are similar to a single-color ELISPOT, including automatic sensitivity adjustment (SmartSpot™) and automatic spot size/intensity gating (AutoGate™) functions for the objective and reliable detection of true spots and eliminating background spots (not antigen induced) and artifacts (*see Note 2*). Details of single-color ELISPOT image analysis are published elsewhere in detail [18, 19], and are beyond the scope of this chapter. The main criterion for the accurate algorithm performance is linear relation between numbers of spots counted and numbers of cells plated per well [20, 21].

Results of the single-color spot counting for each cytokine in four color T-cell FLUOROSPOT are presented on Fig. 2a–c. For a visual control and publications multi-color images for any combinations of channels can be reconstructed by merging individual color images (shown with count overlays on Fig. 2d–f).

3.8 Center of Mass Distance Algorithm for Detection of Dual-, Triple-, and Multi-color Spots

For each detected single-color spot, X – Y coordinates of the center of masses are calculated and recorded. These center of mass coordinates are then compared between all channels, and spots whose Center of Mass Distances (COMD) are less than maximum COMD are paired (considered to be generated by the same cell) (*see Note 3*). To speed up the process, such comparisons are performed in a certain vicinity of the spots and performed in parallel. The algorithm “qualifying”

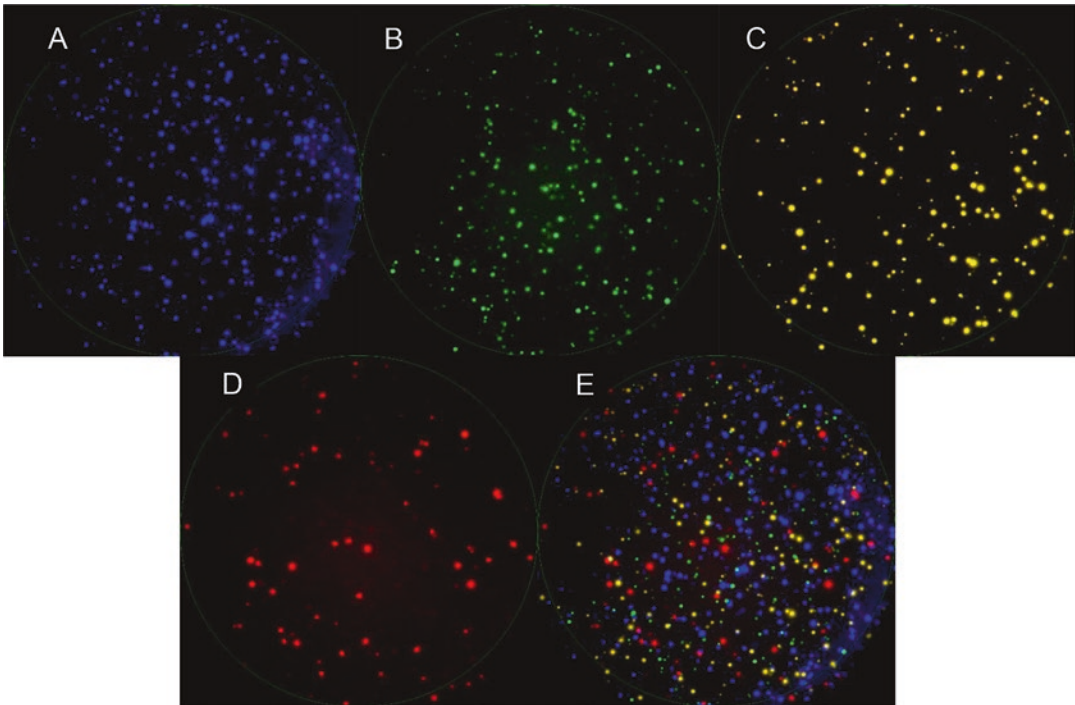


Fig. 1 Capturing of individual color spots in four color human IgG3 (a), IgG1 (b), IgA (c), IgM (d) B-cell FLUOROSPOT assay using individually selectable combinations of the excitation/emission bands (channels). Merged from individual channels four color image is shown in panel e (not used for counting). No cross contamination of fluorescent signals was observed at optimal image capture conditions

spots as dual-/triple-/multi-color is similar to a computer neural network (Fig. 3).

The relations between individual color objects are analyzed based on the maximum COMD parameter and the set of pairing rules. For example, to qualify for a triple-color spot, all distances in the cluster should be inside the COMD (Fig. 4d). To avoid ambiguities in situations when spot of one color (green for example) has the same distance to two different spots of another color (for example, red), the cluster with higher dimension (if a blue spot is also close enough to a green spot) is favored in this case (Fig. 4f). If partially overlapping spots (red on Fig. 4c) were not separated by Spot Separation function, Fluoro-X™ Software calculates “virtual” centers of masses and pairs them to centers of masses of other color spots (green on Fig. 4c) (*see Note 4*). There are other rules for processing unseparated clusters of closely situated spots; together, they guarantee accurate dual-/multi-color spot detection even in crowded wells.

After individual color spots are counted in all channels and paired where appropriate, the single-, dual-, triple-, and multi-color events are generated by the algorithm and all parameters

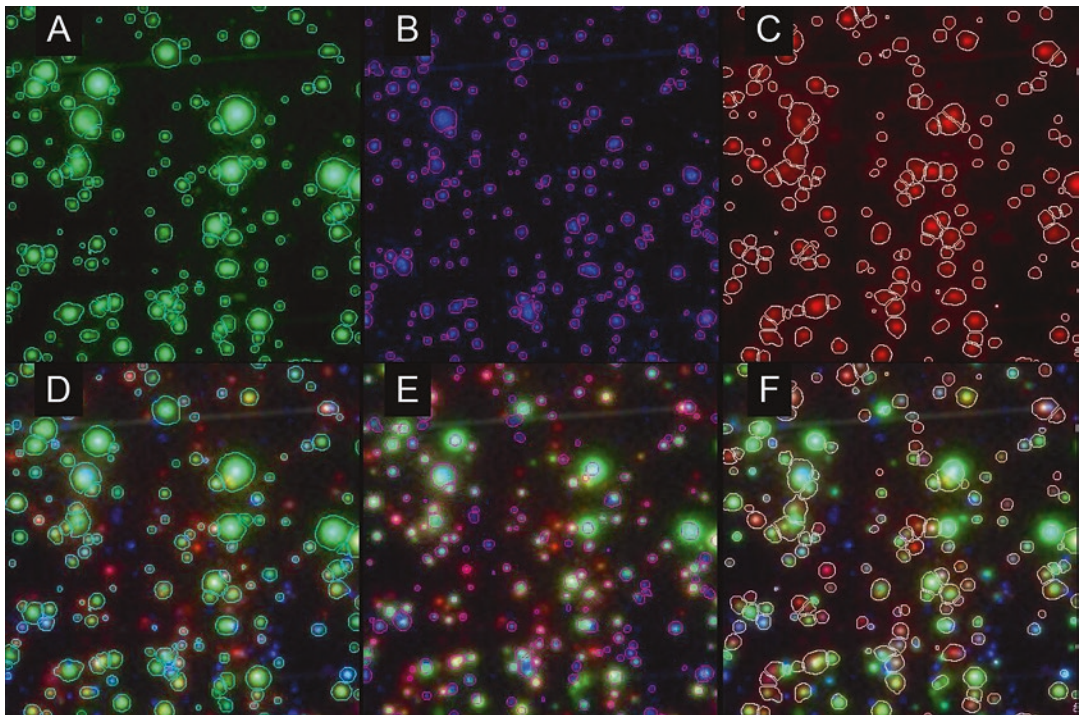


Fig. 2 Counting of individual color spots in the triple-color human IFN- γ (green), TNF- α (blue), and IL-2 (red) T-cell FLUOROSPOT assay. Magnified regions of the well scanned and counted using individual color detection is shown on top panels **a**, **b**, and **c**. Single-color spots count overlays are also shown on the merged triple-color images (bottom panels **d**, **e**, and **f**). Partially overlapping spots were separated by spot separation function of ImmunoSpot® Software

associated with each event are recorded (size, color density, time, etc.). These data can be retrieved (as Flow Cytometry Standard .fcs file) for a *post-hoc* detailed high-content analysis using either Fluoro-X™ Data Management module or any commercial flow cytometry software. The detailed workflow for the multi-color counting using ImmunoSpot® 7.0 Software is presented in [22].

3.9 Validation of Counting Algorithms Using Four Color B-Cell FLUOROSPOT

For the multi-color counting validation, we used four color B-cell FLUOROSPOT assays of human Ig classes/subclasses (IgM, IgA, IgG1, IgG3). Polyclonally pre-activated PBMC [15] were tested in linear titrations using anti- κ/λ chain monoclonal antibodies as a capture reagent and anti-Ig class/subclass detection antibodies. Because individual B cells, due to the allelic exclusion, can only express a single type of Ig molecule, this model is optimally suited for validating multi-color algorithms and for determining frequencies of false positive multi-color spots.

Figure 5 depicts four color FLUOROSPOT for human IgA, IgM, IgG1, and IgG3. The number of individual color spots (for each subtype) closely follows linear relationship to the number of

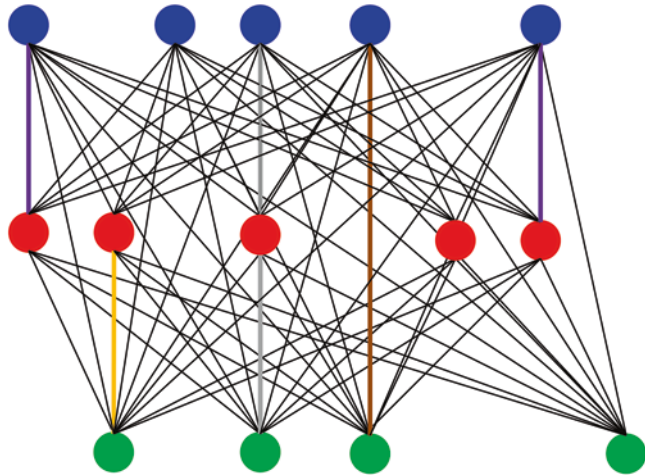


Fig. 3 Spot pairing algorithm for multi-color events generation. Center of mass X–Y coordinates for individual spots of one color (blue for example) are compared to those of other colors (red and green) in certain neighborhood (shown in a single dimension). Every pairwise comparison between individual spots coordinates in blue, red, and green images (or layers) is shown as connecting black line. If the distance between centers of masses of spots in different layer is smaller than COMD, these two spots are paired to form a two color event. Such pairing is shown as violet lines (for blue/red spots), yellow (red/green spots) and brown line (blue/green spots). Gray lines indicate blue/red/green triple-color event

PBMCs plated (panel a), validating the accuracy of the single-color counting algorithm [20, 21]. Slight deviation from the linearity at highest used cell numbers (overcrowded wells with over 1000 spots) results from the large percentage of partially overlapping spot separated by counting algorithm.

Even when no true dual-/multi-color spots were produced (as is the case in Fig. 5), certain number of random overlays of individual color spots giving an appearance of multi-color spots was always observed. In contrast to the genuine spots, the counts of random overlay spot numbers drop in geometrical progression with cell numbers and numbers of colors (Fig. 5b, c). For example for the dual-color situation at highest cell concentration (10,000/well), 1200 green spots and 1400 blue spots resulted in 145 random overlays (about 6%). For half of the cells plated (5000/well) random overlays counts dropped down to 20 (about 2%) and so on. Random triple-color spots overlays are much rarer events: at highest cell numbers used, 1200 green, 1400 blue, and 500 red spots resulted in only 0.2% of triple-color random overlays. Quadruple random overlays were not detectable even at highest cell numbers used. Similar results were obtained among 12 donor

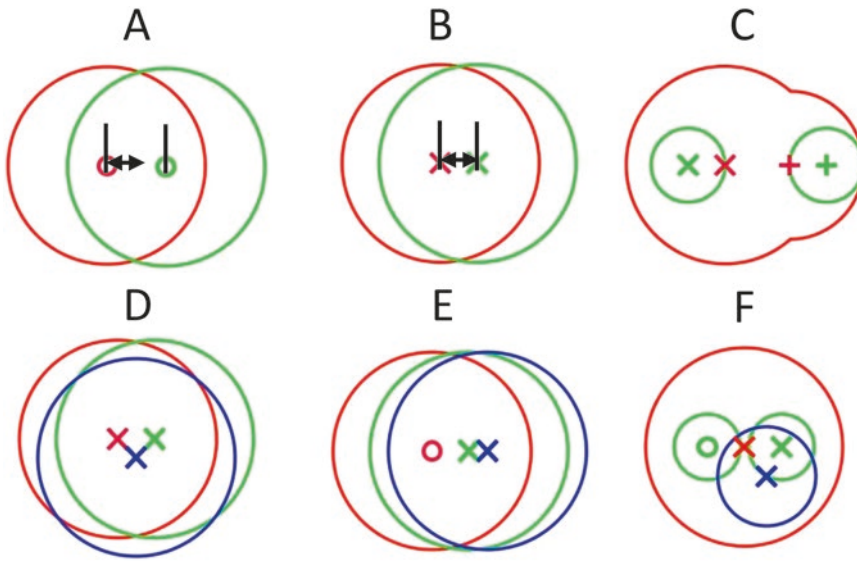


Fig. 4 Spot pairing rules for multi-color events generation are based on the minimal centers of mass distance (COMD). Counting overlays for individual color spots are shown as red, green, and blue circles, and their centers of masses are indicated by “x” (if spots are paired) or “o” if they are not paired. In Panel **a**, the distance between red and green centers is greater than minimal allowed value (shown by double point arrow) and spots are not paired, whereas in **b** it is smaller than/equal to COMD and a two color event (spot) is generated. In **c**—when two overlapping spots (red) are not resolved by spot separation function, “virtual” centers of masses (red crosses) are calculated and two dual-color events are generated. In panel **d**, a triple-color spot is shown with all distances between centers of masses smaller than COMD. In panel **e**, pairing resulted in one green/blue dual-color spot (as indicated by green and blue “x”) and one single-color spot (red “o”). In panel **f**, right green spot (green “x” center) was paired to the blue spot (blue “x”). In this example, red spot center (red “x”) is equidistant from the right green (green “x”)- and the left green (green “o”) spots. In such an instance of equal distances, the algorithm favors higher order events (spots with more colors) resulting in one triple red/green/blue and one single-color green spot. The less favorable alternative would be two dual-color spots (red with left green and blue with right green spot). COMD distances are shown larger in magnitude in the diagram for better visual representation

PBMC samples tested in both three color (Ig class) and four color IgG class/subclass assays (data not shown).

3.10 Statistical Predictions and Scrambled Image Analysis Permit Correction of Random Overlays of Spots

If counting algorithm works properly, the number of “false” dual-/multi-color spots detected in B-cell assays should match theoretical (statistical) predictions for random spot overlays. We used statistical calculations based on the Poisson Point Process to evaluate the effect of such random overlays on the counting results.

Statistical calculations were performed by using both Poisson formula (3) and Monte Carlo simulations (*see* Subheadings 3.4 and 3.5). The results of Monte Carlo simulations closely matched Poisson formula, thus validating the use of latter method for the prediction of “false” positive multi-color spot frequencies (data not shown).

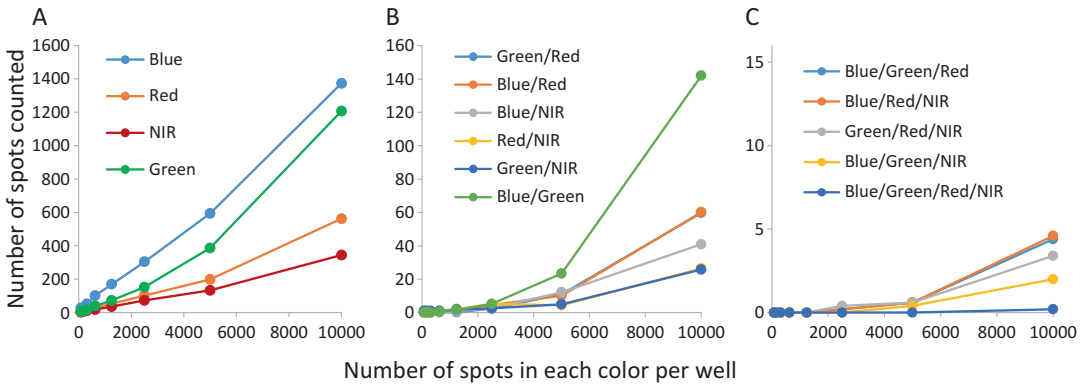


Fig. 5 Frequencies of the random spot overlays in four color B-cell FLUOROSPOT vs. numbers of pre-activated PBMCs plated per well. Panel **a** shows linear relationship between numbers of PBMC plated (X-axis) and the numbers of counted spots (Y-axis) in individual single-color images (labelled: IgG3 as blue, IgA—red, IgG1—green and IgM—near infrared (NIR)). Panel **b** shows numbers of detected random overlay (false positive dual-color spots) for all dual-color combinations plotted vs. numbers of PBMC/well. Panel **c** similarly shows data for three and four color spots. Maximum 145 of false positive two color spots were counted for 1400 blue spots and 1200 green spots (about 6% at COMD = 0.5%). Maximum number of random triple-color spots did not exceed 0.2%. In contrast to the linear function for single-color spots, dual-/triple-color spot numbers dropped in geometrical progression with decreasing cell concentrations plated. False positive four color spots were not detectable even at highest cell numbers

Two independent methods of generating random spot overlays (theoretical Poisson model and scrambled image counts described in Subheading 3.6) (*see Note 5*) exactly matched results of B-cell FLUOROSPOT (Fig. 6), validating the multi-color spot counting algorithm used (*see Note 6*). The monotonicity of the graphs in Fig. 6 (where results for all 6 two color combination are plotted together) proves that frequencies of “false” dual-color spots (actually counted or simulated) do not depend on which two colors are used.

Statistical prediction shows that the number of random overlays grows with the increase of COMD (compare Fig. 6a, b). In the ImmunoSpot® Software, COMD is expressed as percentage of an image vertical size. It makes COMD independent of image pixel size. In case of two colors (shown in Fig. 6) with total 1000 spots of both color per well, COMD equal to 0.5 results in the 19–20 random overlays (about 2%), whereas at COMD equal to 0.75 there will be about 50 random overlays (5%). In practice, the COMD parameter depends mainly on the chromatic aberrations of the optical system (*see Note 7*). Automatic correction for the random overlays implemented in the ImmunoSpot® Software makes precise settings of COMD unnecessary. Minimal value must guarantee detection of all true dual-/multi-color spots (see below) and

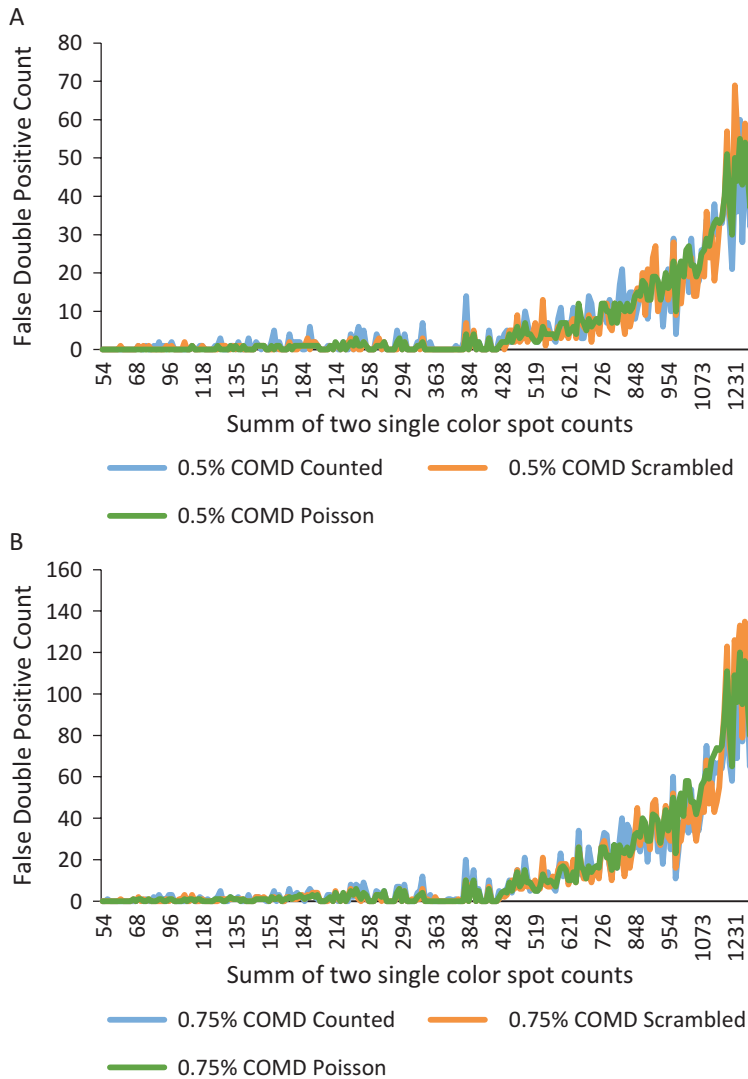


Fig. 6 Statistically predicted and experimentally counted numbers of “false” dual-color spots in four color B-cell FLUOROSPOT (see legend to Fig. 5 for additional details). Two COMD values equal to 0.5% (panel **a**) and to 0.75% (panel **b**) were used for both counting and simulations. Numbers of false positive dual-color spots (Y-axis) are plotted vs. total number of spots in every possible two color combination (X-axis). For example, with COMD 0.5, about 20 “false” dual-color spots resulted from 600 blue and 400 green spots (total 1000 on X-axis) and about 9 “false” dual-color spots resulted from 600 blue and 200 red spots (total 800 on X-axis). With COMD 0.75, the same two combinations resulted in about 50 and 20 “false” dual-color spot counts, respectively. The same PBMC sample shown in Fig. 5 at the same dilutions was used for the experimental counts. The proportion of the individual color spots in every dual-color combinations can be found in Fig. 5a. The blue line reflects results of the experimentally counted dual-color spots, green corresponds to the probabilistic predictions based on Poisson model, and orange line shows results for counting of image with scrambled spot coordinates

maximal value should not result in the numbers of random overlays significantly higher than the numbers of true multi-color spots. Typical values lay between 0.5 and 0.8% of the image size (Fig. 6). For 1000×1000 pixels image, the COMD is in the range of 5–8 pixels. Sometimes cells are moving during the secretion period which may require higher COMD settings.

3.11 Linear Cell Titrations in Four Color FLUOROSPOT Prove Accurate Detection of Polyfunctional T Cell

The use of overlaid multi-color images (shown with counted spots outlines in Fig. 7) enables visual control of multi-color counting for each possible color combination. However the most reliable way to validate true frequencies of dual- or multi-color spots produced by cytokine secreting T cells is to perform serial dilutions of cells. Dual and triple concentric overlays (shown in different color on Fig. 7) indicate dual- and triple-positive spots, respectively.

As demonstrated in the previous section, the frequencies of random spot overlays diminish in the geometrical progression when cells are linearly diluted. The relative frequencies (percentage) of real multi-color spots should stay the same (linearly decreasing with cell dilution). Representative data from such validation study is shown in Fig. 8 utilizing the human IFN- γ /TNF- α /GzB triple-color FLUOROSPOT kit. When counting parameter are set correctly, counted numbers of dual- and triple-color spots perfectly follow linear function validating the accuracy of multi-color counting algorithm. A CD8 cell response of a single A2 restricted donor to CMV peptide pp65 (495–503) is shown in Fig. 8 for all possible color combinations. Experiments were repeated for over 50 donor/antigen combinations using both MHC Class I restricted peptides (CD8 responses) and full protein antigens (CD4 responses). For all responses studied, the relationship between number of dual-/multi-color spots and cell concentrations were uniformly linear (data not shown).

A scientifically validated, accurate, single-color spot counting algorithm is an absolute prerequisite for the accurate multi-color spot recognition in T- and B-cell FLUOROSPOT assay. The use of SmartCount™ and AutoGate™ functions makes single-color spot count objective and user independent (*see Note 2*). ImmunoSpot® single-color counting software has been validated in multiple reported studies including “blind” multi-laboratory studies [23, 24].

The multi-color spot recognition method implemented in ImmunoSpot® Fluoro-X™ Suite is based on the individual single band fluorescent images and Center of Mass Distance pairing algorithm. The ability to create optimal for a given set of fluorescent tags combination of excitation/emission bands maximizes the number of colors which can be analyzed simultaneously and allows for the detection of polyfunctional cytokine producing cells, where

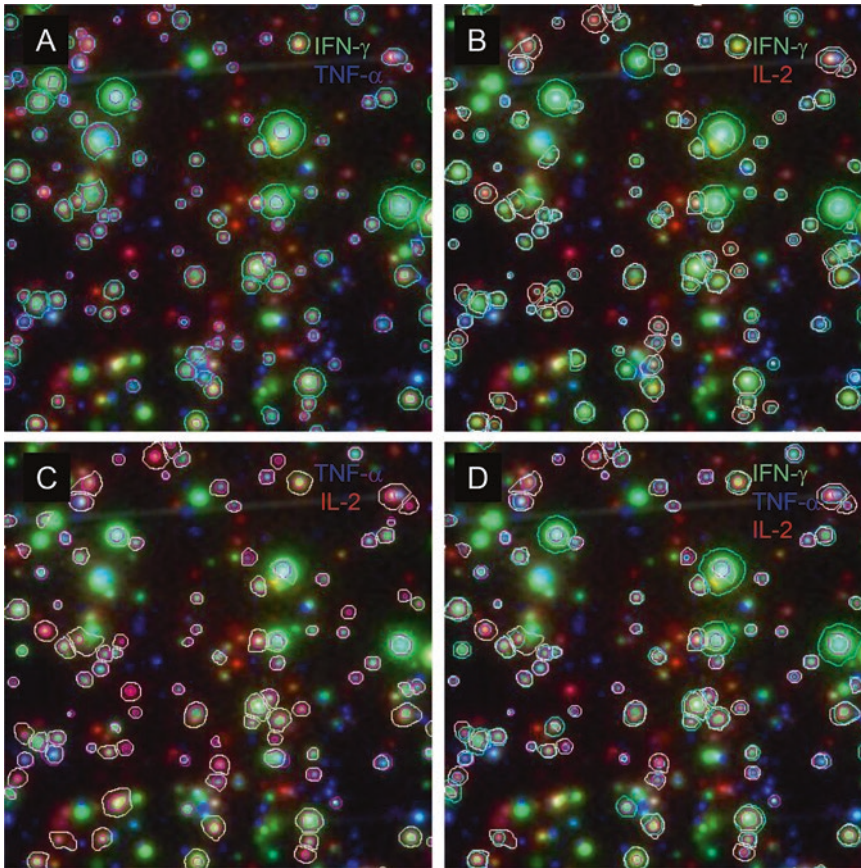


Fig. 7 Counting of dual- and triple-color spots in the human IFN- γ (green), TNF- α (blue), and IL-2 (red) T-cell FLUOROSPOT assay (magnified region of the well is shown). All combinations of two color spot overlays (panels **a**, **b**, and **c**) and triple-color spot overlays (panel **d**) are shown superimposed over the merged triple-color image

the individual cytokine levels produced may be quantitatively different (*see Note 1*). Even significant (hundreds and thousands of times) excess of one analyte will not obstruct the detection of the other/s. Another important advantage of this approach is the selective excitation of one label at a time. This approach eliminates potential bleeding of fluorescent signals emitted by fluorochromes into each other's channels when their emission spectra partially overlap. There is no need for highly selective narrow band filters for close emission spectra resolution, and wide band emission filters can be used for maximizing detection sensitivity. CTL Series 7 Ultimate ImmunoSpot[®] analyzer is capable of resolving up to twelve color fluorescence using commercially available organic fluorochromes in visual spectrum range (400–900 nm) with maximum possible sensitivity.

When pairing spots from individual color images (channels), we allow for certain small distances between their centers of masses

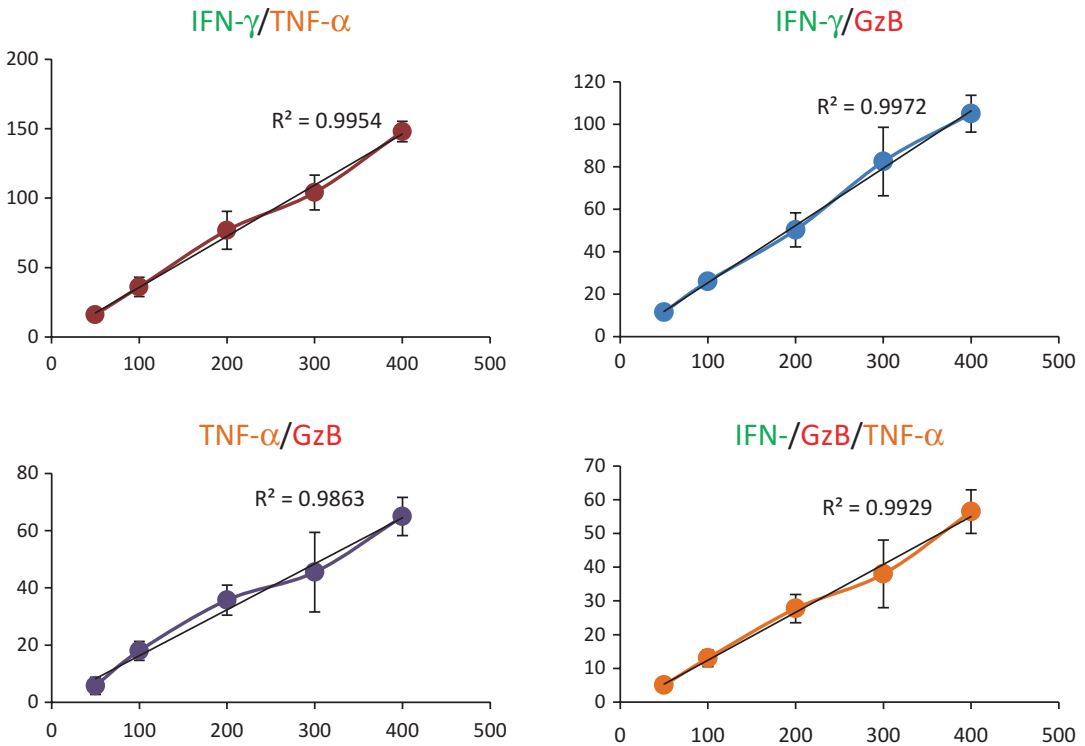


Fig. 8 Validation of the multi-color counting in the triple-color human IFN- γ /TNF- α /GzB assay (see Subheadings 2 and 3). Numbers of dual-/triple-color spots counted in ImmunoSpot® Fluoro-X™ Software (Y-axis) are plotted vs. the numbers of PBMCs plated (shown in thousands on X-axis). Single-color spot counts were performed using SmartSpot™ and AutoGate™ functions with pairing algorithm minimal COMD set to 0.5%. Vertical error bars represent ± 1 SD calculated from four repetitive wells. The linear regression coefficient, R^2 , for all color combinations was close to one reflecting direct linear relationship between the numbers of dual-/triple-color spots and the number of cells plated per well (decreasing cell numbers lead to the proportional reduction of dual-/triple-color spot counts)

(COMD). There are few reasons why centers of spots of different color do not coincide precisely. First is the accuracy of center of mass detection: it is never precise at the microscopic pixel level, particularly with small spots. Second is the chromatic aberration of the optical system: though modern lenses are corrected for chromatic aberrations, there is still some shift in the relative position of spots of different colors. Such minute shift is consistent across all spots in the image for any given scan and can thus be corrected with high confidence. Third reason is cell movement: activated T and B cells can move on the membrane during the secretion period (see Note 3). The probability of movement increases proportionally with the assay incubation time which for IL-17 can be as long as 72 h [25]. If two cytokines are produced by the same cell with different kinetics (like IFN- γ and GzB [26, 27], or IFN- γ and IL-17 [25, 28]), corresponding color spots will be shifted as a

result of such cellular movement. First two factors are constant for a given instrument and color combination, default factory settings for COMD are usually the best. If cell movement is affecting counting results, some increase of COMD could be needed. However, even in this case the COMD settings are constant for a specific analyte combination and do not need to be adjusted each time (*see Note 7*).

Ex vivo frequencies of polyfunctional T cells expressing two and more cytokines could be as low as just a few percent [1–13] which is in the same range as the frequencies of random dual-color spot overlays theoretically predicted for high count wells (starting at about 200–300 individual color spots and geometrically progressing after that). This entails correction for random overlays a mandatory part of any multi-color spot counting algorithm (*see Note 5*). We used two methods to calculate random spot overlays. First is statistical prediction: if cells are randomly distributed over the membrane surface, their positions (X - Y coordinates) have to be distributed according to the Poisson spatial distribution function [16]. Using actual numbers of individual color spots counted per well, ImmunoSpot® Fluoro-X™ Software calculates probabilities for centers of masses of the spots of different colors to be at or closer than COMD using Poisson model. In a second approach, the software counts dual-/triple-/multi-color spots using scrambled images where original relative positions of spots of different colors were randomly modified (*see Subheading 3.6*). Though either method provides practically identical results, both of them are implemented in the ImmunoSpot® Software (*see Note 5*).

Automatic correction for the frequencies of random spot overlays permits pairing algorithm parameters (primarily COMD) vary in wide range without affecting the accuracy of true multi-color spot counts. In principle, once the fluorescent reader, testing reagents, and protocols are tested and optimal counting parameters are established for a given combination of cytokines, validation by serial dilution of cells is not required anymore. We still recommend performing cell titrations for unknown samples/antigen combinations to identify optimal cell concentrations for a given assay.

Another important factor that affects multi-color counting is the partially overlaying of spots. Even in uncrowded wells (50–100 spots), there are certain numbers of doublets, triplets, or rarely, multiples detected (Figs. 1, 2, and 7). If two (or more) partially overlaid spots (of the same color) are detected as a single object, the resultant center of mass will not be correct for either of these spots. If, for example, one of these overlaid spots was of dual-color, the pairing will fail and a dual-positive event will not be generated. Also, a large number of false positive multi-color events may be generated if one single-color cluster is mistakenly paired to another color cluster. Similar to the random overlays, the frequencies of

partially overlapping single-color spots will rise in geometrical progression with the numbers of spots extant per well. ImmunoSpot® Software implements powerful algorithms to separate touching/overlapping spots. In addition, the Fluoro-X™ pairing algorithm is able to calculate “virtual” centers of masses for partially overlapping spots (Fig. 4c) insuring accurate counting even in the crowded wells (*see Note 4*).

Each manufacturer of FLUOROSPOT instruments could present multiple arguments in favor of their hardware and/or software. However, the only way for the user to objectively assess system performance is to conduct a validation study. As discussed earlier, major problems/errors in multi-color counting are spot number dependent. Hence, the best proof of accurate analysis is the direct linear relationship between the numbers of cell plated (single-color spot counts) and the numbers of single-/dual-/multi-color spots detected. Such validation data are presented on Fig. 8 (*see Note 8*). As we demonstrate, the frequency of false positive spots drops in a geometrical progression, while true multi-color spots show a direct linear relationship to the number of cells plated. In this study, using objective corrections for the random spot overlays and intelligent pairing algorithms, we achieve accurate counts (linear spot/cells titrations), even in crowded wells with over a thousand spots for each individual analyte for multi-color T- and B-cell FLUOROSPOT assays (*see Note 9*).

4 Notes

1. Using individual monochromatic images (channels) instead of analyzing multiband color images eliminates the necessity for sophisticated color recognition algorithms and allows using optimal for each fluorochrome combinations of the excitation/emission wavelengths (bands).
2. The use of SmartCount™ and AutoGate™ functions makes single-color spot count objective and user independent. ImmunoSpot® single-color counting Software has been validated in multiple studies.
3. CTL Fluoro-X™ multi-color analysis Suite utilizes individual color spots pairing algorithm based on the maximal allowed Center of Mass Distances between spot centers (COMD) correcting for chromatic aberrations and possible cells movement.
4. The COMD-based algorithm is capable of accurate pairing of partially overlapping spots (spot clusters which were not fully separated) from the single-color images.
5. Correction for the “false” multi-color spots resulting from the random overlay of individual color spots is a mandatory component of the multi-color counting software. Fluoro-X™

Software Suite provides two independent methods for the “random” spots overlay correction based on the statistical probabilities and on the analysis of scrambled experimental images.

6. Analysis of four color B-cell FLUOROSPOT using serial dilutions proves accuracy of random spot overlays correction methods used.
7. The COMD settings are constant for a specific optics and fluorochrome combination and do not need to be adjusted for each assay.
8. Multi-color T- and B-cell FLUOROSPOT analysis using serial cell dilutions is the only way to validate multi-color data analysis system.
9. Direct linear relationship between cell numbers and the numbers of dual-, triple- and quadruple-spots in the four color T-cell FLUOROSPOT fully validates the COMD-based multi-color spot analysis system.

References

1. Zimmerli SC, Harari A, Cellerai C, Vallelian F, Bart PA, Pantaleo G (2005) HIV-1-specific IFN-gamma/IL-2-secreting CD8 T cells support CD4-independent proliferation of HIV-1-specific CD8 T cells. *Proc Natl Acad Sci U S A* 102(20):7239–7244
2. Betts MR, Nason MC, West SM, De Rosa SC, Migueles SA, Abraham J, Lederman MM, Benito JM, Goepfert PA, Connors M, Roederer M, Koup RA (2006) HIV non-progressors preferentially maintain highly functional HIV-specific CD8+ T cells. *Blood* 107(12):4781–4789
3. Almeida JR, Price DA, Papagno L, Arkoub ZA, Sauce D, Bornstein E, Asher TE, Samri A, Schnuriger A, Theodorou I, Costagliola D, Rouzioux C, Agut H, Marcelin AG, Douek D, Autran B, Appay V (2007) Superior control of HIV-1 replication by CD8+ T cells is reflected by their avidity, polyfunctionality, and clonal turnover. *J Exp Med* 204(10):2473–2485
4. Papagno L, Almeida JR, Nemes E, Autran B, Appay V (2007) Cell permeabilization for the assessment of T lymphocyte polyfunctional capacity. *J Immunol Methods* 328(1–2):182–188
5. Day CL, Mkhwanazi N, Reddy S, Mncube Z, van der Stok M, Klennerman P, Walker BD (2008) Detection of polyfunctional Mycobacterium tuberculosis-specific T cells and association with viral load in HIV-1-infected persons. *J Infect Dis* 197(7):990–999
6. Duvall MG, Precopio ML, Ambrozak DA, Jaye A, McMichael AJ, Whittle HC, Roederer M, Rowland-Jones SL, Koup RA (2008) Polyfunctional T cell responses are a hallmark of HIV-2 infection. *Eur J Immunol* 38(2):350–363
7. Hutnick NA, Carnathan D, Demers K, Makedonas G, Ertl HC, Betts MR (2010) Adenovirus-specific human T cells are pervasive, polyfunctional, and cross-reactive. *Vaccine* 28(8):1932–1941
8. Owen RE, Heitman JW, Hirschhorn DF, Lanteri MC, Biswas HH, Martin JN, Krone MR, Deeks SG, Norris PJ, NIAID Center for HIV/AIDS Vaccine Immunology (2010) HIV+ elite controllers have low HIV-specific T-cell activation yet maintain strong, polyfunctional T-cell responses. *AIDS* 24(8):1095–1105
9. Akinsiku OT, Bansal A, Sabbaj S, Heath SL, Goepfert PA (2011) Interleukin-2 production by polyfunctional HIV-1-specific CD8 T cells is associated with enhanced viral suppression. *J Acquir Immune Defic Syndr* 58(2):132–140
10. El Fenniri L, Toossi Z, Aung H, El Iraki G, Bourkkadi J, Benamor J, Laskri A, Berrada N, Benjouad A, Mayanja-Kizza H, Betts MR, El Aouad R, Canaday DH (2011) Polyfunctional Mycobacterium tuberculosis-specific effector memory CD4+ T cells at sites of pleural TB. *Tuberculosis* 91(3):224–230
11. Han Q, Bagheri N, Bradshaw EM, Hafler DA, Lauffenburger DA, Love JC (2012)

- Polyfunctional responses by human T cells result from sequential release of cytokines. *Proc Natl Acad Sci U S A* 109(5):1607–1612
12. Samri A, Bacchus-Souffan C, Hocqueloux L, Avettand-Fenoel V, Descours B, Theodorou I, Larsen M, Saez-Cirion A, Rouzioux C, Autran B, ANRS VISCONTI study group (2016) Polyfunctional HIV-specific T cells in post-treatment controllers. *AIDS* 30(15):2299–2302
 13. Smith SG, Zelmer A, Blitz R, Fletcher HA, Dockrell HM (2016) Polyfunctional CD4 T-cells correlate with in vitro mycobacterial growth inhibition following *Mycobacterium bovis* BCG-vaccination of infants. *Vaccine* 34(44):5298–5305
 14. Kuerten S, Batoulis H, Recks MS, Karacsony E, Zhang W, Subbramanian RA, Lehmann PV (2012) Resting of cryopreserved PBMC does not generally benefit the performance of antigen-specific T cell ELISPOT assays. *Cell* 1(3):409–427
 15. Pinna D, Corti D, Jarrossay D, Sallusto F, Lanzavecchia A (2009) Clonal dissection of the human memory B-cell repertoire following infection and vaccination. *Eur J Immunol* 39(5):1260–1270
 16. Kingman JFC (1993) Poisson processes, Oxford studies in probability, vol 3. Clarendon Press, New York
 17. Kroese DP, Taimre T, Botev ZI (2011) Handbook of Monte Carlo methods. Wiley, New York
 18. Lehmann PV (2005) Image analysis and data management of ELISPOT assay results. *Methods Mol Biol* 302:117–132
 19. Zhang W, Lehmann PV (2012) Objective, user-independent ELISPOT data analysis based on scientifically validated principles. *Methods Mol Biol* 792:155–171
 20. Karulin AY, Caspell R, Dittrich M, Lehmann PV (2015) Normal distribution of CD8+ T-cell-derived ELISPOT counts within replicates justifies the reliance on parametric statistics for identifying positive responses. *Cell* 4(1):96–111
 21. Karulin AY, Karacsony K, Zhang W, Targoni OS, Moldovan I, Dittrich M, Sundararaman S, Lehmann PV (2015) ELISPOTs produced by CD8 and CD4 cells follow log normal size distribution permitting objective counting. *Cell* 4(1):56–70
 22. Megyesi Z, Lehmann PV, Karulin AY (2018) Multi-color FLUOROSPOT counting using ImmunoSpot® Fluoro-X™ suite. In: Kalyuzhny AE (ed) Handbook of ELISPOT, Methods in molecular biology, 3rd edn. Springer, New York
 23. Zhang W, Caspell R, Karulin AY, Ahmad M, Haicheur N, Abdelsalam A, Johannesen K, Vignard V, Dudzik P, Georgakopoulou K, Mihaylova A, Silina K, Aptsiauri N, Adams V, Lehmann PV, McArdle S (2009) ELISPOT assays provide reproducible results among different laboratories for T-cell immune monitoring--even in hands of ELISPOT-inexperienced investigators. *J Immunotoxicol* 6(4):227–234
 24. Sundararaman S, Karulin AY, Ansari T, BenHamouda N, Gottwein J, Laxmanan S, Levine SM, Loffredo JT, McArdle S, Neudoerfl C, Roen D, Silina K, Welch M, Lehmann PV (2015) High reproducibility of ELISPOT counts from nine different laboratories. *Cell* 4(1):21–39
 25. Wunsch M, Zhang W, Hanson J, Caspell R, Karulin AY, Recks MS, Kuerten S, Sundararaman S, Lehmann PV (2015) Characterization of the HCMV-specific CD4 T cell responses that are associated with protective immunity. *Virus* 7(8):4414–4437
 26. Nowacki TM, Kuerten S, Zhang W, Shive CL, Kreher CR, Boehm BO, Lehmann PV, Tary-Lehmann M (2007) Granzyme B production distinguishes recently activated CD8(+) memory cells from resting memory cells. *Cell Immunol* 247(1):36–48
 27. Kuerten S, Nowacki TM, Kleen TO, Asaad RJ, Lehmann PV, Tary-Lehmann M (2008) Dissociated production of perforin, granzyme B, and IFN-gamma by HIV-specific CD8(+) cells in HIV infection. *AIDS Res Hum Retrovir* 24(1):62–71
 28. Duechting A, Przybyla A, Kuerten S, Lehmann PV (2017) Delayed activation kinetics of Th2- and Th17 cells compared to Th1 cells. *Cell* 6(3)



Multi-Color FLUOROSPOT Counting Using ImmunoSpot® Fluoro-X™ Suite

Zoltán Megyesi, Paul V. Lehmann, and Alexey Y. Karulin

Abstract

Multi-color FLUOROSPOT assays for simultaneous detection of several T-cell cytokines and/or classes/sub-classes of immunoglobulins secreted by B cells have recently become a major new avenue of development of ELISPOT technology. Advances in assay techniques and the availability of commercial test kits stimulated development of multi-color FLUOROSPOT data analysis platforms. The ImmunoSpot® Fluoro-X™ Software Suite was developed by CTL as an integrated data acquisition, analysis, and management solution for automated high-throughput processing of multi-color T- and B-cell FLUOROSPOT assay plates. The Fluoro-X™ software counting module is based on SmartSpot™/AutoGate™ technologies and utilizes CTL's Center of Mass Distance algorithm for the detection of multi-color spots. The Fluoro-X™ software provides an objective, user error-free means for analyzing multi-color FLUOROSPOT data. An integrated quality control module, with optional GLP and CFR Part 11 compliant package and role-based security, enables data validation, review, and approval with complete audit trails. The extensive multi-format data output and presentation capabilities of the Fluoro-X™ software allow further analysis of FLUOROSPOT data using any commercial flow cytometry software and facilitate the generation of professional reports and presentation. In this article, we present a detailed step-by-step workflow for the analysis of a human four-color IFN- γ , IL-2, TNF- α , and GzB antigen-specific T-cell assay using the Fluoro-X Software Suite.

Key words T cell, B Cell, Cytokines, Immunoglobulins, Antibodies, ELISPOT, FLUOROSPOT, Multiplex, Multi-Color, Spot counting, Objective, Center of mass, AutoGate™, SmartSpot™, SmartCount™ Quality Control, Software, Fluoro-X™, Fluorescence, Label

1 Introduction

Over past decade, ELISPOT has become the gold standard for monitoring T- and B-cell immunity in clinical trials. This is primarily to its capacity for single cell resolution, high throughput, and ability to detect antigen-specific responses directly *ex-vivo*. Recent advances in multi-color fluorescent spot detection made FLUOROSPOT a fast-developing method for simultaneous measurements of up to seven analytes at a time [1]. Whereas the main criteria for objective, user independent single color ELISPOT counting are well established [2, 3], and commercial analysis